East European Journal of Physics. 1. 428–446 (2026)
DOI: 10.26565/2312-4334-2026-1-51 ISSN 2312-4334

NUMERICAL INVESTIGATION OF HEAT TRANSFER ANALYSIS USING ELECTROMAGNETOHYDRODYNAMICS WITH AGGREGATED NANOPARTICLES

A. Lokeshwari, **Peri K. Kameswaran***
Department of Mathematics, School of Advanced Sciences, Vellore Institute of Technology, Vellore 632014, India
Corresponding Author e-mail: perikamesh@gmail.com,
Received October 22, 2025; revised January 8, 2026; accepted January 11, 2026

Optimizing heat transmission remains a significant contemporary challenge in modern technological applications. Nanofluids exhibit strong potential thermal conductivity for enhancing heat transfer and improving energy system efficiency. In comparison to dispersed nanoparticles, aggregated nanoparticles are noteworthy for evaluating the thermal behavior of nanoparticles at the nanoscale. In spite of that aggregation effect, the fractal dimension of the aggregated nanoparticles will have a transformative effect on heat transfer. The objective of the present study is to investigate the influence of electromagnetohydrodynamic effects on heat transfer in a nanofluid containing aggregated nanoparticles over an exponentially stretching sheet. The governing equations for momentum and energy are transformed into a system of nonlinear ordinary differential equations with specified boundary conditions. An analytical solution is presented for a specific instance where the electric field parameter is absent. Numerical solutions are achieved for various ranges of physical parameters, and computed results are validated with existing literature. The findings indicate that nanoparticle aggregation leads to thickening the thermal boundary layer and improving heat transfer. In addition to this synergistic effect of aggregation and electric field, it leads to the decrease in velocity profiles. At 5% volume fraction, aggregated nanoparticles provide a heat transfer enhancement of approximately 34% over dispersed nanoparticles. The temperature profiles exhibit a rising trend with an increasing volume fraction. In the presence of aggregated nanoparticles, both the skin friction coefficient and the Nusselt number increase with rising magnetic field strength.

Keywords: *Aggregated nanoparticles; Electric field; Magnetic field; Radiation; Viscous dissipation; Exponential stretching sheet*

PACS: 04.50.Kd, 04.20.Jb

1. INTRODUCTION

Over the past several decades, research has been designed for various experimental setups and methodologies to analyze how aggregation influences nanofluid behavior and to develop methods for controlling aggregation to optimize its thermal performance. Nanoparticles aggregation occurs in which individual particles stick together and form a cluster. Numerous factors have been involved in this phenomenon like, interaction between nanoparticles, Van der Waals forces, surface charges (Lee et al. [1]), etc. Aggregated nanoparticles (especially metals like platinum, gold, silver, or iron oxides) are widely used as catalysts, inks for printing electrical circuits, and removal of contaminants from water due to their high surface area-to-volume ratio.

Gaganpreet and Srivastava [2] examined the influence of viscosity and thermal conductivity of aggregated nanoparticles in a nanofluid. They found that as the size of the aggregated spherical nanoparticles increases, exactly for radii $r_a = 3r, 4r, 5r$ the viscosity also increases. Liao et al. [3] studied nanoparticles aggregation on the thermal conductivity of nanofluid by molecular dynamic solutions. They observed a particle size is a key factor to determine the potential mechanisms that affect the thermal conductivity of nanofluid. Feng et al. [4] investigated the effective thermal conductivity of nanofluid based on the structure of nanolayer and nanoparticles aggregation. Their study reveals that nanoparticles aggregation has an effective thermal conductivity even at lower volume fractions. Mahanthesh [5] investigated the study of the flow and heat transport of aggregation kinematics of nanoparticles with quadratic radiative heat flux using a modified Buongiorno model. They figured out that the magnitude of velocity is higher in the case of strong convective heating.

Experimental studies have shown that aggregated nanoparticles can increase the efficiency of heat conductivity in comparison to the dispersed particle. Aggregated nanoparticles can enhance heat transfer in nanofluid through their unique structure, which forms conductive networks or pathways. This can significantly improve the thermal conductivity and convective heat transfer properties. Chen et al. [6] studied the experimental and theoretical study of aggregated nanoparticles and their thermal radiation properties. They have experimentally validated their results, showing that aggregated nanoparticles exhibit more effective heat transfer compared to individual nanoparticles. Motevasel et al. [7] studied the heat conductivity of four types of nanofluids containing aggregated nanoparticles and also compared their results with experimental validation. They analyzed that the nanoparticle's aggregation has a better attribution of heat conductivity even at low volume concentration. Muhammad et al. [8] have reported that the aggregative and non-aggregative effects of nanofluid flow in the application of cooling systems in liquid rocket engines. They found the aggregative and non-aggregative nanoparticle flows are similar for both velocity and temperature profiles for particular cases; however, noticeable differences emerged at higher values of radiation and volume fraction. Pang et al. [9] analyzed the nanoparticles

Cite as: A. Lokeshwari, P.K. Kameswaran, East Eur. J. Phys. 1, 428 (2026), https://doi.org/10.26565/2312-4334-2026-1-51

aggregation model for heat conduction mechanism in nanofluid. They concluded that the interfacial thermal resistance and nanolayer have minimal impact on the thermal conductivity, even if nanoparticles concentration is very minimal. Numerous researchers Ellahi et al. [10], Sathya and Naveen [11] studied the role of aggregation and non-aggregation effects of nanoparticles in determining the thermal behavior of nanofluids. They found that the aggregation effects of nanoparticles have a better efficiency of heat transfer compared to individual nanoparticles.

Electromagnetohydrodynamics is the study of fluid flow influenced by both electric and magnetic fields. EMHD flows are especially relevant in microfluidics, cooling systems, spacecraft thermal control, and biomedical devices, where external electric and magnetic fields are used to control fluid movement at small scales. Duraihem [12] targeted the EMHD Darcy–Forchheimer flow of Sutterby nanofluid over a stretching sheet using the finite difference approach. Ramesh et al. [13] explored the EMHD flow of hybrid nanofluid flow over an exponential stretching sheet. They resulted that the velocity distribution is strengthened with increasing Helmholtz–Smoluchowski velocity, whereas the temperature distribution exhibits a diminishing trend. Loganayagi and Kameswaran. [14] investigated the effects of an electromagnetic field and heat source/sink on two-dimensional nanofluid flow over a stretching cylinder. Their findings indicate that Gadolinium is particularly suitable for thermomagnetic generators due to its optimal operating temperature range. Madhu et al. [15] scrutinized the impacts of nanoparticles aggregation across a stretching sheet with an analytical solution. Their study explores how the aggregation state of nanoparticles influences heat transfer efficiency and highlights its significant role in thermal conductivity with the influence of porous medium. Swain et al. [16] conducted a study to investigate the influence of aggregated nanoparticles on radiative 3D flow of Maxwell fluid over a permeable stretching surface.

In addition to the above considered effects, it is interesting to study the effects of thermal radiation due to its applications. When nanofluids are employed, the presence of nanoparticles can alter the radiative heat transfer characteristics by modifying the absorption, scattering, and emission properties of the base fluid. Kameswaran et al. [17] examined the radiation effects on MHD flow over an exponential stretching sheet and also found analytical solutions using hyper-geometric functions, highlighting the significant role of radiation in modifying the thermal boundary layer behavior. It is evident that thermal radiation enhances the temperature within the boundary layer region. Wang et al. [18] studied the effects of thermal radiation and nanoparticles aggregation on the gap between cone and disk. Consequently, the phenomenon of nanoparticle aggregation has been extensively examined by various researchers such as Rajput et al. [19], Ali et al. [20], and Rafique et al. [21] across diverse scientific and engineering domains.

Only a limited study has generalized the effects of nanoparticle aggregation in the existing literature. Madhu et al. [15] investigated the influence of nanoparticle aggregation and porous media on flow over an exponential stretching sheet, without considering the effects of magnetic and electric fields. Kameswaran et al. [17] examined the role of thermal radiation on hydromagnetic newtonian fluid flow over an exponential stretching sheet, neglecting both nanoparticle aggregation and electric field effects. Motivated by these limitations, the present study investigates the impact of aggregated and non-aggregated nanoparticles on heat transfer in electromagnetohydrodynamic (EMHD) flow over an exponential stretching sheet, incorporating the combined effects of electric and magnetic fields, thermal radiation, and viscous dissipation. The results are presented graphically to illustrate and compare the heat transfer characteristics of nanofluids with and without nanoparticle aggregation. The research questions are formulated based on the discussion of how nanoparticle aggregation influences the flow and heat transfer characteristics of EMHD nanofluids.

- How does the aggregation of nanoparticles affect the thermal fields?
- How does induction of nanoparticle aggregation by an electric field impact both the flow dynamics and thermal behavior of nanofluids?
- How do aggregated and non-aggregated nanoparticles affect EMHD flow over an exponential stretching sheet?
- How do electric and magnetic fields, thermal radiation, and viscous dissipation influence the behavior of nanofluid flow and heat transfer?

2. MATHEMATICAL MODEL

We consider the steady, incompressible, laminar, two-dimensional electromagnetohydrodynamic flow of a viscous liquid over an exponentially stretching sheet. The geometric representation of the flow model is illustrated in Fig. 1.

- Assume the origin is positioned at the slit, with the plate extending along the x-axis.
- The sheet's velocity is modeled as an exponential function of the distance x, where $U_w = U_0 e^{\frac{x}{L}}$, with U being the velocity at the slit and L a characteristic length.
- The fluid temperature is denoted by T, while T_w represents the wall temperature and T_∞ denotes the ambient temperature of the sheet, which is assumed constant, where $T_w = T_\infty + T_0 e^{\frac{2x}{L}}$.
- A uniform electric field $E(x)$ and magnetic field of intensity $B(x)$ are simultaneously applied, both oriented perpendicular to the flow direction.

- Moreover, a modified Krieger-Dougherty model and a Maxwell-Bruggeman [5] model were used for aggregated nanoparticle viscosity and thermal conductivity, respectively.

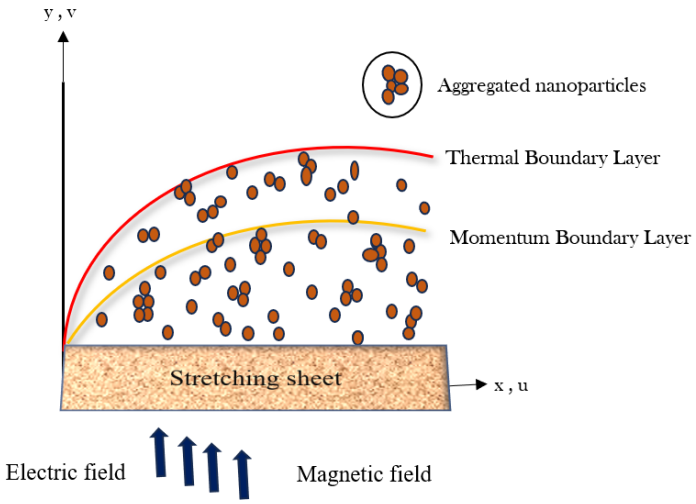

Figure 1. Structural diagram of the model

2.1. Mathematical formulation

Based on the following assumptions, the corresponding system of mathematical equations is formulated as follows: (Kameswaran et al. [17])

$$\frac{\partial u}{\partial x}+\frac{\partial v}{\partial y}=0, \tag{1}$$

$$u\frac{\partial u}{\partial x}+v\frac{\partial v}{\partial y}=\frac{\mu_{nf}}{\rho_{nf}}\left(\frac{\partial^2 u}{\partial y^2}\right)+\frac{\sigma_{nf}}{\rho_{nf}}\left(EB-B^2u\right), \tag{2}$$

$$u\frac{\partial T}{\partial x}+v\frac{\partial T}{\partial y}=\frac{K_{nf}}{(\rho C_p)_{nf}}\left(\frac{\partial^2 T}{\partial y^2}\right)-\frac{1}{(\rho C_p)_{nf}}\left(\frac{\partial q_r}{\partial y}\right)+\frac{\sigma_{nf}}{(\rho C_P)_{nf}}(uB-E)^2 + \frac{\nu_f}{(C_p)_f}\left(\frac{\partial u}{\partial y}\right)^2. \tag{3}$$

The boundary conditions for the Eqs. (1)-(3) are as follows:

$$u=U_w=U_0e^{\frac{x}{L}},\quad v=0,\quad T=T_w=T_\infty+T_0e^{\frac{2x}{L}},\quad \text{at}\quad y=0. \tag{4}$$

$$u\to 0,\qquad T\to T_\infty,\qquad as\quad y\to\infty. \tag{5}$$

Here, the velocity component u along the x direction and the velocity component v along the y direction respectively.

Following Rosseland's approximation, q_r is the heat-radiation flux,

$$q_r=-\frac{4\sigma^*}{3k^*}\frac{\partial T^4}{\partial y}, \tag{6}$$

Here σ^* represents the Stefan-Boltzman constant and k^* denotes a mean absorption coefficient. The term is T^4 linearized by expanding about the ambient temperature T_∞. Using Taylor series expansion and neglecting higher-order terms, we approximate $T^4\cong 4T_\infty^3T-3T_\infty^4$.

Introducing a stream function $\psi(x,y)$ such that,

$$u=\frac{\partial\psi}{\partial y}\quad\text{and}\quad v=-\frac{\partial\psi}{\partial x},$$

The stream function is identically satisfying Eq. (1).

The following similarity variables are taken into account for the exponential stretching sheet problem and are defined as follows: (Mabood et al. [22]).

$$u = U_0 e^{\frac{x}{L}} f_\eta(\eta), \quad v = -\left(\frac{\nu_f U_0}{2L}\right)^{\frac{1}{2}} e^{\frac{x}{2L}} [f(\eta) + \eta f_\eta(\eta)],$$
$$T = T_\infty + T_0 e^{\frac{2x}{L}} \theta(\eta), \quad \eta = \left(\frac{U_0}{2\nu_f L}\right)^{\frac{1}{2}} y e^{\frac{x}{2L}}, \tag{7}$$

Here, the dimensionless stream function is referred to as $f(\eta)$ and the dimensionless temperature is referred to as $\theta(\eta)$ and η is referred to as a similarity variable. Using Eq. (7), the Eq. (1) gets satisfied and Eq. (2)-(3) is transformed into an ordinary differential equations as described below:

$$\left(\frac{Z_1}{Z_2}\right) f_{\eta\eta\eta} - 2f_\eta^2 + f f_{\eta\eta} + \left(\frac{Z_3}{Z_2}\right)[M(E - f_\eta)] = 0, \tag{8}$$
$$\left(\frac{Z_4}{Z_5}\right)\frac{\theta_{\eta\eta}}{Pr} + \frac{4}{3}R\frac{\theta_{\eta\eta}}{Pr}\left(\frac{1}{Z_5}\right) + \theta_\eta f - 4f_\eta\theta + \left(\frac{Z_3}{Z_5}\right) MGb\left(f_\eta - E\right)^2 + Gbf_{\eta\eta}^2 = 0, \tag{9}$$

along with the boundary conditions,

$$f(0) = 0, \quad f_\eta(0) = 1, \quad \lim_{\eta\to\infty} f_\eta(\eta) = 0$$
$$\theta(0) = 1, \quad \lim_{\eta\to\infty} \theta(\eta) = 0. \tag{10}$$

The dimensionless parameters emerging in Eqs. (8)-(9) are stated below,

$$M = \frac{2\sigma_f B_0^2 L}{\rho_f U_0}, \quad R = \frac{4\sigma^* T_\infty^3}{k^* k_f}, \quad E = \frac{E_o}{U_0 B_0}, \quad Pr = \frac{\nu_f(\rho C_p)_f}{k_f},$$
$$Gb = \frac{U_0^2}{(C_p)_f T_0}, \quad Z_1 = \frac{\mu_{nf}}{\mu_f}, \quad Z_2 = \frac{\rho_{nf}}{\rho_f}, \quad Z_3 = \frac{\sigma_{nf}}{\sigma_f}, \quad Z_4 = \frac{K_{nf}}{K_f},$$
$$Z_5 = \frac{(\rho C_P)_{nf}}{(\rho C_P)_f}.$$

The viscosity of the base fluid is defined as μ_f, the density of the base fluid is indicated as ρ_f and the density of the nanofluid is denoted as ρ_{nf}. K_{nf} indicates a thermal conductivity of the nanofluid while k_f is referred to as the thermal conductivity of the base fluid. The specific heat capacity of the nanofluid is represented as $(\rho C_P)_{nf}$ and the specific heat capacity of the base fluid is denoted as $(\rho C_P)_f$, the solid volume portion of the nanofluid is indicated as ϕ, the dynamic viscosity is referred as μ_{nf}. The density of nanofluid is assumed to be ρ_{nf}. The symbol for thermal conductivity and heat capacity of nanofluid are represented as K_{nf} and $(\rho C_p)_{nf}$.

2.2. Effective Thermophysical properties of Nanofluid

Viscosity and thermal conductivity are two thermophysical properties of nanofluid that are influenced by the cluster of nanoparticles in the fluid. In the case where the impact of nanoparticles aggregation is insignificant, the effective dynamic viscosity and thermal conductivity were calculated using the modified Brinkman and Maxwell models (Makhdoum et al. [23]).

2.3. Aggregated nanoparticles parameters

Thermophysical properties are designated in accordance with the aggregation behavior of nanoparticles. The nanoparticle measurement results coincided precisely after taking into account the aggregation component of the nanoparticle. The

Table 1. Thermophysical properties of Copper and Water (Swain et al. [16])

Nanoparticle	$\rho(kg/m^3)$	$C_p(J/kgK)$	$\sigma(s/m)$	$k(W/mK)$	Prandtl number
Copper (Cu)	8933	385	$5.8 * 10^7$	401	-
Water H_2O	997.1	4179	0.05	0.613	5.83

symbol ϕ_{agg} is signed as an aggregated nanoparticle volume fraction and it is defined as $\phi_{agg} = \phi\left(\frac{R_{agg}}{R_p}\right)^{3-D_f}$. Here R_{agg} indicates the radius of the aggregated nanoparticle and R_p refers to the radius of the individual dispersed nanoparticle. D_f is termed as a fractal index, where D_f=1.8, $\frac{R_{agg}}{R_p} = 3.34$, $\phi_m = 0.605$, $\eta = 2.5$. The constants used in the present study are referred from: [Mahanthesh [5], Swain et al. [16]].

The Modified Krieger-Dougherty model and the modified Maxwell model are utilized to account for nanoparticle aggregation in thermal conductivity and effective viscosity as seen in Table 3. The thermal conductivity of the aggregated term is coined as (k_a), where,

$$\frac{k_a}{k_f} = \frac{1}{4}[(3\phi_{int}-1)\frac{k_s}{k_f} + (3(1-\phi_{int})-1) + [((3\phi_{int}-1)\frac{k_s}{k_f} + (3(1-\phi_{int})-1))^2 + 8\frac{k_s}{k_f}]^{\frac{1}{2}}] \text{ where, } \phi_{int} = \left(\frac{R_{agg}}{R_p}\right)^{D_f-3}$$

Here, the subscripts s and f are figured as nanofluid and fluid, respectively.

2.4. Effect of Electromagnetic Field on Nanoparticle Aggregation

The electromagnetic field influences nanoparticle aggregation by altering interparticle forces and particle motion. Specifically, the magnetic field produces Lorentz forces that suppress fluid velocity and Brownian motion, increasing the likelihood of particle–particle collisions and aggregation. In addition, the electric field induces electrophoretic motion and particle polarisation, leading to dipole–dipole attractions that further influence on aggregate formation. The role of the electromagnetic field is manifested indirectly through its influence on the flow dynamics via the Lorentz force. The modified velocity field directly impacts the transport of momentum and thermal energy. Simultaneously, the presence of nanoparticle aggregation alters the effective thermophysical properties, such as viscosity, thermal conductivity, and electrical conductivity. These effective properties determine the strength of the electromagnetic body force, which subsequently governs the overall flow and heat transfer performance.

2.5. Skin friction and Heat transfer Coefficients

The skin friction coefficient quantifies frictional losses and energy dissipation in fluid flow, and it is governed by fluid viscosity, flow velocity, surface roughness, and boundary layer behavior.

Table 2. Thermophysical properties of nanofluid without aggregation (Mackolil et al. [24])

Properties	Without Aggregation
Dynamic Viscosity	$\frac{\mu_{nf}}{\mu_f} = \frac{1}{(1-\phi)^{2.5}}$
Density	$\frac{\rho_{nf}}{\rho_f} = (1-\phi) + \phi\frac{\rho_s}{\rho_f}$
Electrical Conductivity	$\frac{\sigma_{nf}}{\sigma_f} = 1 + \frac{3\left(\frac{\sigma_s}{\sigma_f}-1\right)\phi}{\left(\frac{\sigma_s}{\sigma_f}+2\right)-\left(\frac{\sigma_s}{\sigma_f}-1\right)\phi}$
Thermal Conductivity	$\frac{k_{nf}}{k_f} = \frac{(k_s+2k_f)-2\phi(k_f-k_s)}{(k_s+2k_f)+\phi(k_f-k_s)}$
Specific heat capacity	$\frac{(\rho C_P)_{nf}}{(\rho C_P)_f} = (1-\phi) + \phi\frac{(\rho C_P)_s}{(\rho C_P)_f}$

Table 3. Thermophysical properties of nanofluid with aggregation (Rawat et al. [25] and Rana et al. [26])

Properties	With Aggregation
Dynamic Viscosity	$\frac{\mu_{nf}}{\mu_f} = \left(1-\frac{\phi_{agg}}{\phi_m}\right)^{(-\eta)\phi_m}$
Density	$\frac{\rho_{nf}}{\rho_f} = \left(1-\phi_{agg}\right) + \phi_{agg}\left(\frac{\rho_s}{\rho_f}\right)$
Electrical Conductivity	$\frac{\sigma_{nf}}{\sigma_f} = 1 + \frac{3\left(\frac{\sigma_s}{\sigma_f}-1\right)\phi_{agg}}{\left(\frac{\sigma_s}{\sigma_f}+2\right)-\left(\frac{\sigma_s}{\sigma_f}-1\right)\phi_{agg}}$
Thermal Conductivity	$\frac{k_{nf}}{k_f} = \frac{(k_a+2k_f)-2\phi_{agg}(k_f-k_a)}{(k_a+2k_f)+\phi_{agg}(k_f-k_a)}$
Specific heat capacity	$\frac{(\rho C_P)_{nf}}{(\rho C_P)_f} = \left(1-\phi_{agg}\right) + \phi_{agg}\frac{(\rho C_P)_s}{(\rho C_P)_f}$

The Skin friction coefficient is expressed as follows:

$$C_f = \frac{2\tau_w}{\rho_f U_w^2}, \tag{11}$$

where τ_w represents the shearing stress at the wall surface due to fluid motion, and it is defined as:

$$\tau_w = -\mu_{nf}\left[\frac{\partial u}{\partial y}\right]_{y=0} = -\mu_{nf}\left[\frac{U_0}{L}\sqrt{\frac{Re}{2}}\right] e^{\frac{3x}{2L}} f_{\eta\eta}(0) \tag{12}$$

Here, μ_{nf} denotes the dynamic viscosity coefficient, and the Reynolds number is represented as $Re = \frac{LU_0}{\nu}$

By using Eq. (12) in Eq. (11) we obtain,

$$(Re)^{0.5} C_f = -\left(\frac{Z_1}{Z_2}\right)\sqrt{2} f_{\eta\eta}(0) \tag{13}$$

The Nusselt number is a key dimensionless parameter used in heat exchanger design, offering insights into optimizing system performance by quantifying the enhancement in heat transfer due to fluid motion. The Nusselt number is expressed as follows:

$$Nu_L = \frac{L}{K_f}\left(\frac{q_w}{T_w - T_\infty}\right) \tag{14}$$

The rate of heat transfer in terms of thermal flux at the wall is expressed as:

$$q_w = -K_{nf}\left[\frac{\partial T}{\partial y}\right]_{y=0} = -K_{nf}\left[\frac{T_w - T_\infty}{L}\sqrt{\frac{Re}{2}}\right] e^{\frac{x}{2L}}\theta_\eta(0) \tag{15}$$

here K_{nf} is referred as the coefficient of Thermal conductivity of the fluid. By using Eq. (15) in Eq. (14) we obtain,

$$(Re)^{-0.5} Nu_L = -(Z_4/\sqrt{2})\theta_\eta(0) \tag{16}$$

3. EXACT SOLUTION

For particular case in which the absence of an electric field, the governing momentum and energy equations reduce to simplified forms.
i.e., $E \to 0$, Eq. (8) and Eq. (9) along with boundary conditions are compressed by

$$\frac{Z_1}{Z_2} f_{\eta\eta\eta} + f f_{\eta\eta} - 2f_\eta^2 - \frac{Z_3}{Z_2} M f_\eta = 0, \tag{17}$$

$$\left(\frac{Z_4}{Z_5}\right)\frac{\theta_{\eta\eta}}{Pr} + \frac{4}{3}R\frac{\theta_{\eta\eta}}{Pr}\left(\frac{1}{Z_5}\right) + \theta_\eta f - 4f_\eta\theta + \left(\frac{Z_3}{Z_5}\right) M G_b f_\eta^2 + G_b f_{\eta\eta}^2 = 0, \tag{18}$$

along with the boundary conditions,

$$\begin{aligned} &f(0) = 0, \quad f_\eta(0) = 1, \quad f_\eta(\infty) \to 0, \\ &\theta(0) = 1, \quad \theta(\infty) \to 0. \end{aligned} \tag{19}$$

3.1. Momentum equation

Integrating Eq. (17) with η once over to the interval $[0, \eta]$, we obtain

$$\frac{Z_1}{Z_2} f_{\eta\eta} + f f_\eta - \int_0^\eta \left[3f_\eta^2 + \frac{Z_3}{Z_2} M f_\eta\right] d\eta + S = 0, \tag{20}$$

Using boundary conditions, where $\eta \to [0, \infty)$ we obtain and

$$\begin{aligned} S &= -\frac{Z_1}{Z_2} f_{\eta\eta}(0), \\ S &= \int_0^\infty \left[3f_\eta^2 + \frac{Z_3}{Z_2} M f_\eta\right] d\eta, \end{aligned} \tag{21}$$

Once again Integrating Eq. (20), we attain,

$$\frac{Z_1}{Z_2} f_\eta + \frac{1}{2} f^2 = \int_0^\eta \left[\int_0^\eta \left[3 f_\eta^2 + \frac{Z_3}{Z_2} M f_\eta \right] d\eta \right] d\eta - S\eta + \frac{Z_1}{Z_2}, \tag{22}$$

Now, the solution procedure of Eq. (22) may be reduced to the sequential solutions.

$$\frac{Z_1}{Z_2} f_\eta^{(n)} + \frac{1}{2} f^{(n)2} = RHS[f_\eta^{(n-1)}], \tag{23}$$

The Eq. (21) can be solved by introducing an appropriate zero-order approximation as $f_\eta^{(0)}(\eta)$ for $f_\eta(\eta)$. This substitution simplifies the problem, effectively transforming it into a sequence of Riccati-type differential equations. As a result, the overall solution procedure becomes an iterative process, where each step involves solving a Riccati equation with updated approximations based on the previous iteration.

We assume a zero-order approximation as,

$$f(\eta) = \frac{1 - e^{-S\eta}}{S} \tag{24}$$

where S is a parameter associated with nanoparticle volume fraction. Integrating Eq. (24) with respect to η we get,

$$\begin{aligned} f_\eta(\eta) &= e^{-S\eta} \\ f_{\eta\eta} &= -S e^{-S\eta} \end{aligned} \tag{25}$$

After finding the derivatives of Eq. (24) substituting in the Eq. (21), the estimated value of S can be obtained as

$$S = \sqrt{\frac{3}{2} + \frac{Z_3}{Z_2} M}, \qquad S = -\frac{Z_1}{Z_2} f_{\eta\eta}^{(0)}(0) \tag{26}$$

Replacing all the derivatives from the zero-order approximation on the right-hand side of the Eq. (22), the equation for the first-order iteration is formulated as follows:

$$\frac{Z_1}{Z_2} f_\eta^{(n)} + \frac{1}{2} f^{(n)2} = \frac{Z_1}{Z_2} + \frac{3}{4S^2}[e^{-2S\eta} - 1] + \frac{Z_3}{Z_2}\frac{M}{S^2}[e^{-S\eta} - 1] \tag{27}$$

Additionally, we assume that the first-order approximation of f satisfies to the boundary conditions. Consequently,the nonlinear Riccati-type equation can be expressed using the confluent hypergeometric Whittaker function.

3.2. Energy Equation

By introducing this new variable, [See Kameswaran et al. [17]]

$$\xi = \frac{-Pr}{S^2} e^{-S\eta} \tag{28}$$

After finding derivatives of Eq. (28) and substituting into Eq. (18) and takes the form of

$$\xi\theta_{\xi\xi}\left[Z_4 + \frac{4}{3}R\right] + \theta_\xi\left[Z_4 + \frac{4}{3}R - \frac{Pr}{S^2}Z_5 - \xi Z_5\right] + 4\theta Z_5 = \frac{-G_b}{Pr}\left[Z_3 M + Z_5 S^2\right]\xi S^2 \tag{29}$$

the temperature boundary condition are modified into,

$$\theta\left(-\frac{Pr}{S^2}\right) = 1, \qquad \theta(0) = 0. \tag{30}$$

The solution for Eq. (29) is assumed in the form of $\theta(\xi) = \theta_c(\xi) + \theta_p(\xi)$,
where $\theta_c(\xi)$ and $\theta_p(\xi)$ represent complementary and particular solutions. The complementary solution of Eq. (29) indicates a confluent hypergeometric equation(Kummer's function).

$$\theta_c(\xi) = a_0 \xi^\alpha M\left[\alpha - 4, \alpha + 1, \frac{-\xi}{\lambda_2}\right] \tag{31}$$

here $\lambda_2 = Z_4 + \left(\frac{4}{3}\right) R$, $\lambda_3 = Z_5$, $\alpha = Pr^* \left(\frac{\lambda_3}{\lambda_2}\right)$,
where $Pr^* = \frac{Pr}{S^2}$ is the modified Prandtl number.
The particular solution is obtained in the form of

$$\theta_p(\xi) = A\xi^2 + B\xi^3 + C\xi^4, \tag{32}$$

where,

$$A = -\left(\frac{Gb}{Pr^*}\right) \frac{Z_3 M + Z_5 S^2}{4\lambda_2 - 2Pr^* Z_5},$$

$$B = \frac{-2A}{9\lambda_2 - 3Pr^* Z_5},$$

$$C = \frac{-B}{16\lambda_2 - 4Pr^* Z_5},$$

By applying the boundary conditions, the solution is obtained and expressed in terms of the relevant variable, we get,

$$\theta(\eta) = a_0 \frac{e^{S\eta\alpha} M\left[\alpha - 4, \alpha + 1, -\alpha e^{-S\eta}\right]}{M\left[\alpha - 4, \alpha + 1, -\alpha\right]} + APr^{*2} e^{-2S\eta} - BPr^{*3} e^{-3S\eta} + CPr^{*4} e^{4S\eta}, \tag{33}$$

where, $a_0 = 1 - APr^{*2} + BPr^{*3} - CPr^{*4}$.

4. MATHEMATICAL DEMONSTRATION

The governing equations Eqs. (8)-(9) along with the boundary conditions (10) are solved numerically using MATLAB-bvp4c. The MATLAB function bvp4c is used to numerically solve highly nonlinear boundary-value problems. The following parameters are defined as follows:

$$f = y_1, \quad f' = y_2, \quad f'' = y_3, \quad \theta = y_4, \quad \theta' = y_5. \tag{34}$$

Hence by using Eq. (34), the above system of ordinary differential equations from Eqs. (8)-(9) is determined as follows,

$$y_3' = \frac{Z_2}{Z_1}\left[2y_2^2 - y_1 y_3 - \frac{Z_3}{Z_2} M\left(E - y_1\right)\right] \tag{35}$$

$$y_5' = \frac{Z_5}{Z_4 + \frac{4}{3}R}\left[Pr\left(4y_2 y_4 - y_1 y_5 - \left(\frac{Z_3}{Z_5}\right) Gb\left(M(y_2 - E)^2\right) + Gby_3^2\right)\right] \tag{36}$$

The boundary conditions now to be transformed into,

$$y_1(0) = 0, \quad y_2(0) = 1, \quad y_3(0) = A_3, \quad y_4(0) = 1, \quad y_5(0) = A_5 \tag{37}$$

where A_3 and A_5 are considered as intial guess values for the transformations.

5. VALIDATION OF TABULAR RESULTS

From Table 4 and Table 5, it is observed that the present results show good agreement with existing results of (Kameswaran et al. [17]). Table 6 shows that skin friction values for with aggregation and without aggregation of nanoparticles.

6. DISCUSSION OF GRAPHICAL RESULTS

In this problem, we have concentrated on the effects of various pertinent physical parameters on velocity profile ($f(\eta)$), temperature profile ($\theta(\eta)$), skin friction (C_f), and heat transfer rate (Nu_L) with and without Aggregation effect from Figs. (3)-(15). The impact of the magnetic parameter on the velocity distribution is found in Fig. 3 for Cu/H_2O nanofluid. The range of magnetic field is chosen between the values of $0 \leq M \leq 3$. The impact of the magnetic parameters is intensified in the EMHD flow, resulting in a decrease in velocity for both cases of presence and absence of aggregation effects of nanoparticles. This occurs due to the resistive force known as the Lorentz force, where the magnetic field lines are inclined with respect to the electromagnetic force that disturbs the nanofluid flow over an exponentially stretching sheet. The results concluded that in the presence of the aggregation effect, the velocity reduces for increasing the range of magnetic parameters. This happens because aggregated nanoparticles stick together to form clustered structures through hydrodynamic force and appear larger in size compared to dispersed nanoparticles, and this will lead to reducing the speed of flow, and larger aggregated nanoparticles also have more drag, and this force slows down the fluid movement, which

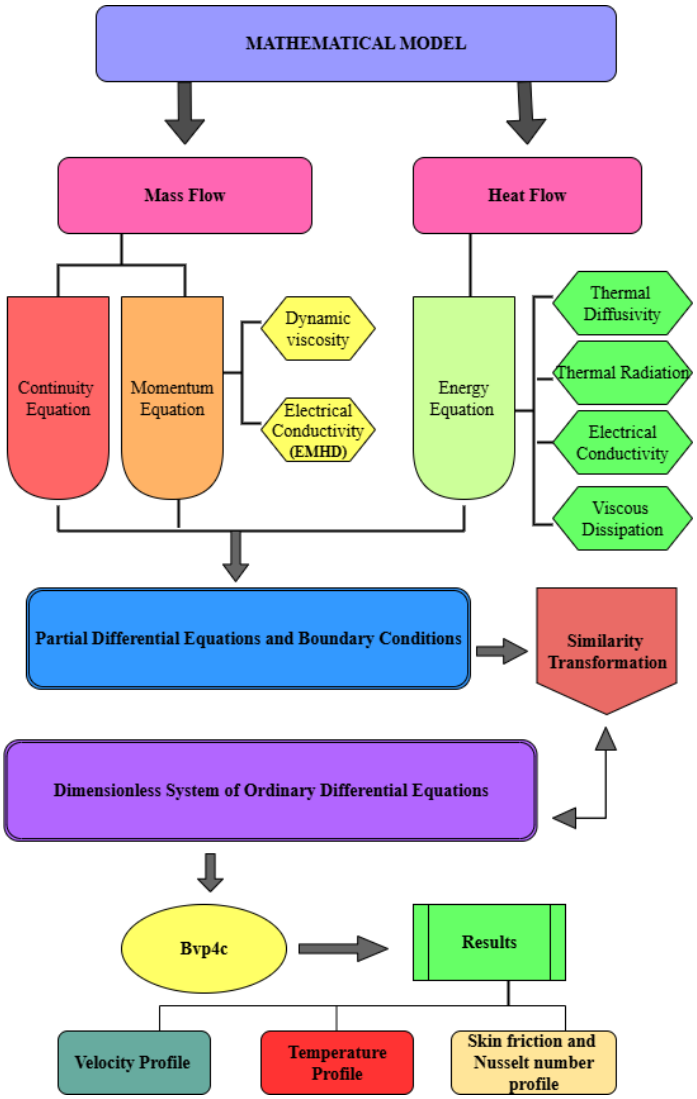

Figure 2. Demonstration of Mathematical model

Table 4. Values of $-f_{\eta\eta}(0)$ are confirmed with Kameswaran et al. [17] for distinct values of M and for fixed values of $E = Pr = R = Gb = 0$

M	Kameswaran et al. [17]	Current results
0	1.28181	1.28181
1	1.62918	1.62918
2	1.91262	1.91262
3	2.15874	2.15874
4	2.37937	2.37937
5	2.58113	2.58113

leads to decreasing the velocity. As a result, aggregated nanoparticles slow down the fluid behavior in the boundary layer region.

Fig. 4 reveals the influence of magnetic parameters on the temperature profile. The temperature rises for both cases while increasing the range of magnetic field parameters. This is because of when magnetic fields are applied to nanoparticles, which results in greater heat buildup especially near heated surfaces in stretching sheets. Generally aggregated nanoparticles can have stronger magnetic interactions; therefore, they can trap more heat. In this case, aggregated nanoparticles can form thermal bridges between the particles, which facilitate better heat transfer compared to non-aggregated nanoparticles.

Table 5. Values of $-\theta_\eta(0)$ are confirmed with Kameswaran et al. [17] for fixed values $M = 1, E = 0, Pr = 7, Gb = 0.2$ of varying values of R

R	Kameswaran et al. [17]	Current results
0	4.55621	4.55621
0.5	3.48315	3.48315
1	2.90580	2.90580
2	2.26050	2.26050
3	1.88981	1.88981

Table 6. Skin friction values $-f_{\eta\eta}(0)$ for with and without aggregation for different parameters

M	E	R	ϕ	Gb	Without Aggregation	With Aggregation
0					1.31521	1.40339
1					1.65638	1.73038
2					1.9366	2.00296
3					2.18066	2.24216
	10^{-3}				1.65638	1.73038
	10^{-4}				1.65704	1.73038
	10^{-5}				1.65711	1.7311
		1			1.65638	1.73038
		1.5			1.65638	1.73038
		2			1.65638	1.73038
		2.5			1.65638	1.73038
			0.01		1.65638	1.73038
			0.02		1.68197	1.79393
			0.03		1.70538	1.82495
			0.05		1.72672	1.82703
				0.1	1.65638	1.73038
				0.5	1.65638	1.73038
				1	1.65638	1.73038
				1.5	1.65638	1.73038

The results of the electric parameter on the velocity distribution are clearly demonstrated in Fig. 5. The Electric parameters are selected within the interval of 10^{-3} to 10^{-5}. From the graph, it is noticed that the flow decelerates for both aggregated and non-aggregated nanoparticles. As we applied the electric field to fluid, the nanoparticles have some interaction between the electric and magnetic fields that can create complex forces between them, and these complex forces generally affect the speed of the fluid flow. If the range of electric parameters increases, the aggregated nanoparticles have different electrophoretic mobility compared to the individual nanoparticles in electric field distribution within the fluid. Hence, aggregated nanoparticles have greater resistance to flow, which can slow the velocity of the fluid.

The outcomes of the electric parameter on the temperature profile are illustrated in Fig. 6. It is observed that the temperature profile increases for both cases of presence and absence of aggregation. When an electric field is applied to the nanofluid, it generates heat, and it is observed that the temperature increases more. From the graph, we conclude that heat transfer is enhanced by the aggregation effect. When aggregated nanoparticles form interparticle contacts and create a region of higher energy density and significant thermal resistance. The region of high thermal resistance can cause the temperature to increase more rapidly with aggregated nanoparticles compared with dispersed nanoparticles.

The temperature patterns for varying the values of the radiation parameter are examined through Fig. 7 with the presence and absence of aggregated nanoparticles. The range of radiation parameters is taken between $1 \leq R \leq 2.5$. The radiation parameter characterizes the relative contribution of the convective heat transfer coefficient to the thermal radiation transfer coefficient. As the radiation value increases, the temperature profile increases more in the presence of aggregated nanoparticles. This means that nanoparticles with aggregation form a structure with cavities or highly irregular geometries that may concentrate radiation on certain things because of localized resonant effects. This results in localized heating to strengthen the temperature gradients and leads to thickening of the thermal boundary layer. When the nanoparticles

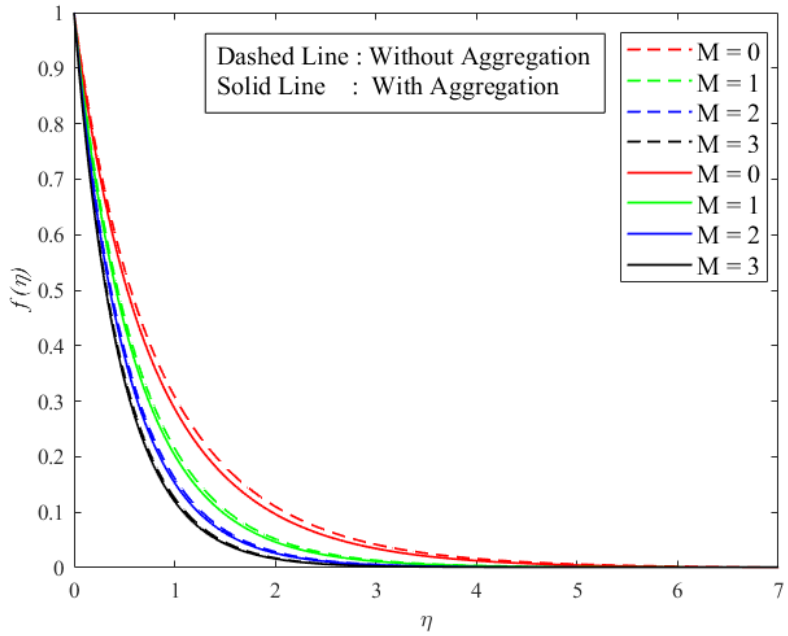

Figure 3. Variation of magnetic parameter on velocity profile for fixing other parameters are $E = 10^{-3}, R = 1, Pr = 5.83, \phi = 0.01, Gb = 0.2$.

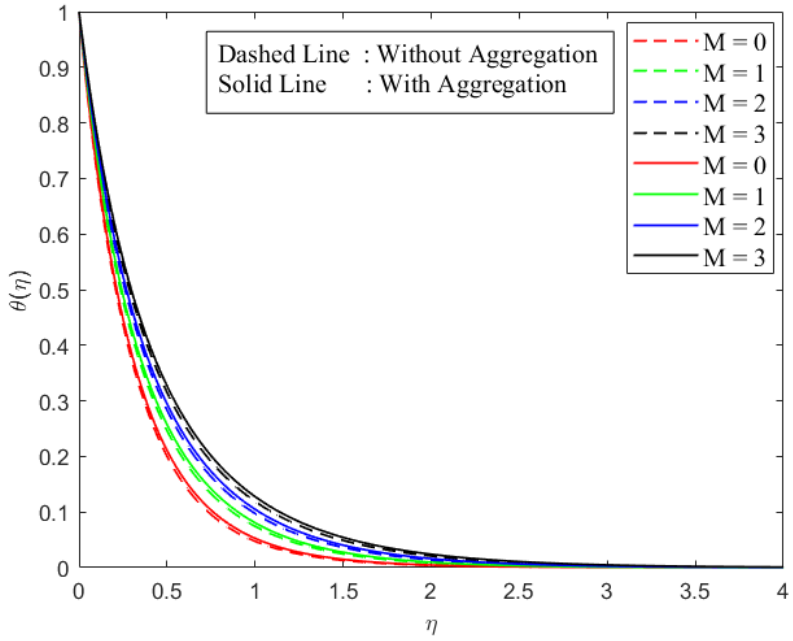

Figure 4. Variation of magnetic parameter on temperature profile for $E = 10^{-3}, R = 1, Pr = 5.83, \phi = 0.01, Gb = 0.2$.

aggregate into clusters, the multiple scattering plays a significant influence in absorbing and scattering radiation due to the small gaps between the aggregated nanoparticles, and both absorption and scattering are enhanced greatly in the near infrared.

Fig. 8 expresses the relationship between the volume fraction of the solids of velocity profile. The range volume fraction is considered between 1% to 4%. The graph represents that aggregated nanoparticles have a greater velocity profile than that of dispersed nanoparticles. The boundary layer can be affected differently by aggregated nanoparticles than by dispersed nanoparticles. In certain instances, aggregation can cause a more prominent velocity gradient close to the wall, as they can act like larger particles, causing more friction and resistance to flow near the boundary. The Krieger-Dougherty model can be utilized to describe the viscosity of the suspension, resulting in an increase in effective viscosity with volume

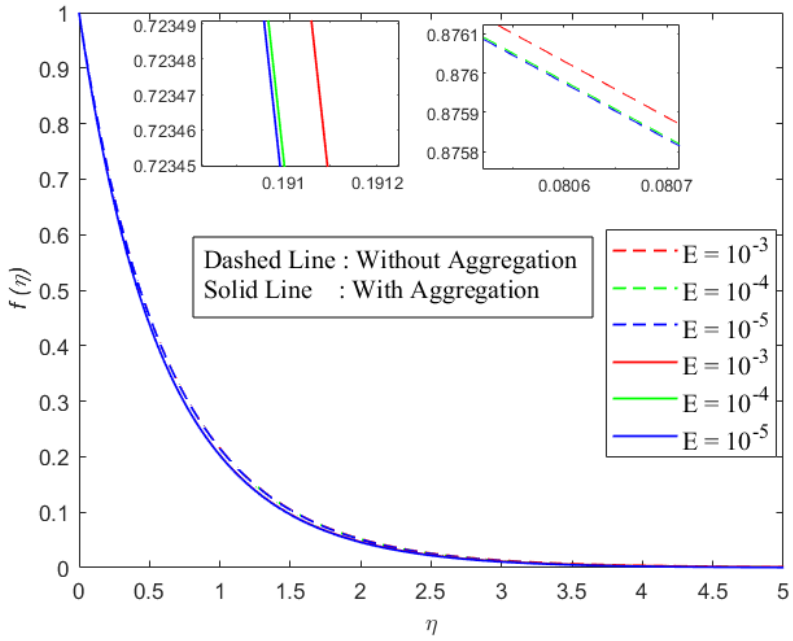

Figure 5. Variation on electric parameter on velocity profile for $M = 1, R = 1, Pr = 5.83, \phi = 0.01, Gb = 0.2$.

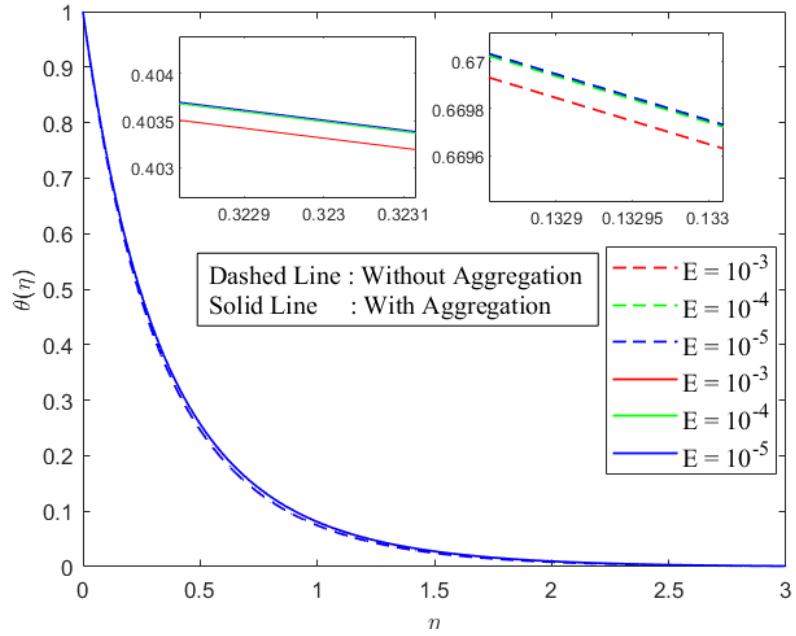

Figure 6. Variation on electric parameter on temperature profile for $M = 1, R = 1, Pr = 5.83, \phi = 0.01, Gb = 0.2$.

fraction. As a result, the velocity profile has a more decreasing sequence in the presence of aggregated nanoparticles.

The effects of the volume fraction on the temperature profile are exemplified in Fig. 9 in both cases of with and without aggregation. The efficiency of heat transfer is directly correlated with the volume fraction of nanoparticles. It is recognized that higher volume fractions of nanoparticles facilitate more heat transfer efficiently in the presence of aggregated nanoparticles than dispersed nanoparticles. This is due to aggregated nanoparticles leading to a higher surface area for heat exchange between the fluid and the nanoparticles; the total surface area of these aggregated particle could be larger than the individual nanoparticles. By increasing its surface area, the aggregated nanoparticles can absorb more heat from the surrounding fluid and enhance their thermal absorption capacity.

Fig. 10 illustrates the influence of accelerated rates of the Gebhart number on the temperature distribution. The range of viscous dissipation considered here is 0.1 to 1.5. The viscous dissipation parameter relates to the process by which the

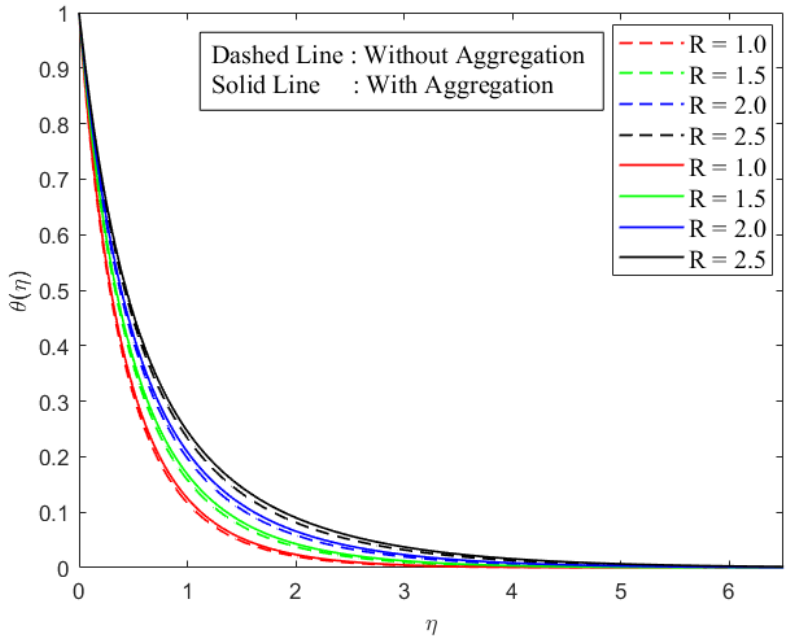

Figure 7. Variation of radiation parameter on temperature profile for $M = 1, E = 10^{-3}, Pr = 5.83, \phi = 0.01, Gb = 0.2$.

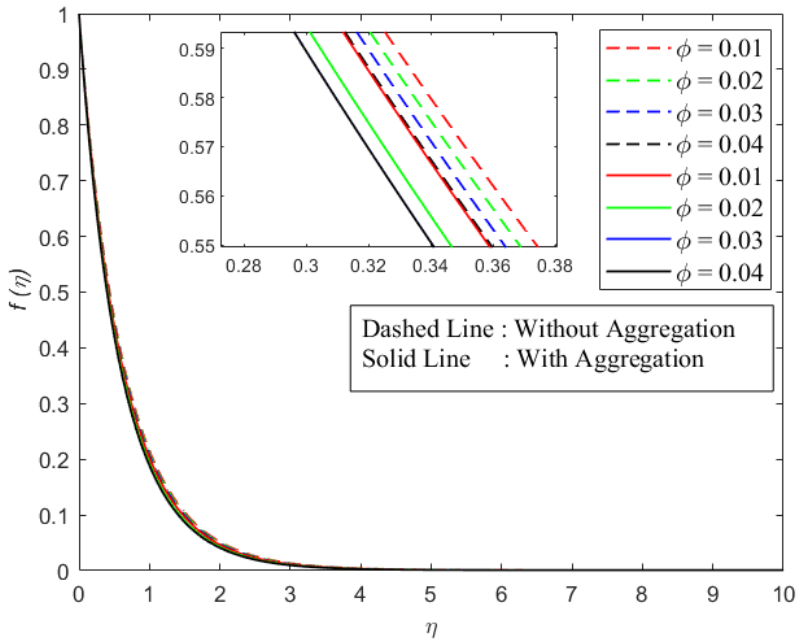

Figure 8. Variation of volume fraction on velocity profile for $M = 1, E = 10^{-3}, R = 1.5, Pr = 5.82, Gb = 0.2$.

fluid friction (mechanical energy) is transformed into heat (thermal energy) due to the internal friction (fluid viscosity) between the fluid layers. From this graph, it is clearly seen that the temperature increase strengthens the values for viscous dissipation parameter with aggregated nanoparticles. The aggregation of nanoparticles increases the effective viscosity of the nanofluid, thereby intensifying internal friction, leading to localized internal heat generation near boundaries. As a result, the combined effect of nanoparticles aggregation and viscous heating can be considered in the design and optimization of high-performance thermal systems.

The behavior of the skin friction coefficient with varying volume fraction and magnetic parameters is illustrated in Fig. 11 for both aggregated and non-aggregated nanoparticles. It is observed that the skin friction coefficient decreases monotonically with an increase in the magnetic parameter in both cases. This happens because the clustered nanoparticles make the fluid more viscous, which enhances the effective viscosity and momentum diffusion within the boundary layer. The

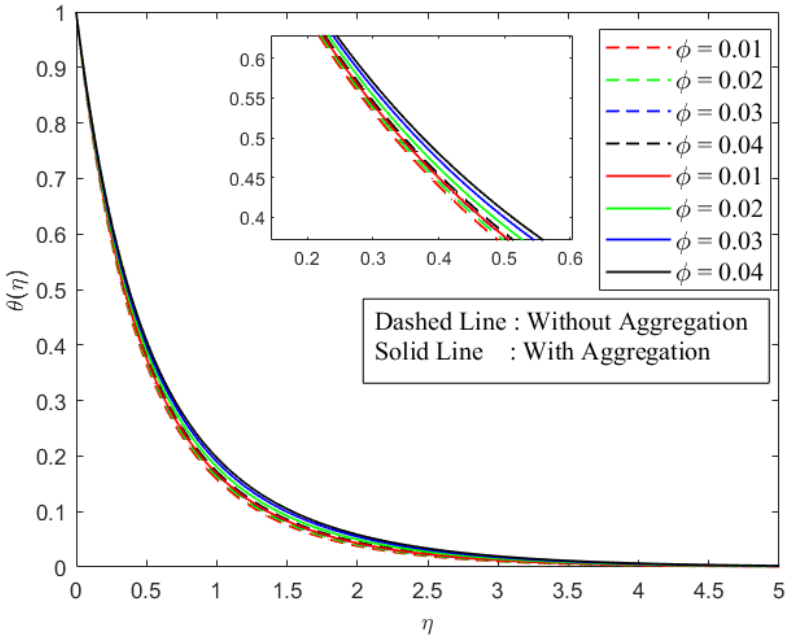

Figure 9. Variation of volume fraction parameter on temperature profile for $M = 1,\ E = 10^{-3},\ R = 1.5,\ Pr = 5.83,$ $Gb = 0.2$.

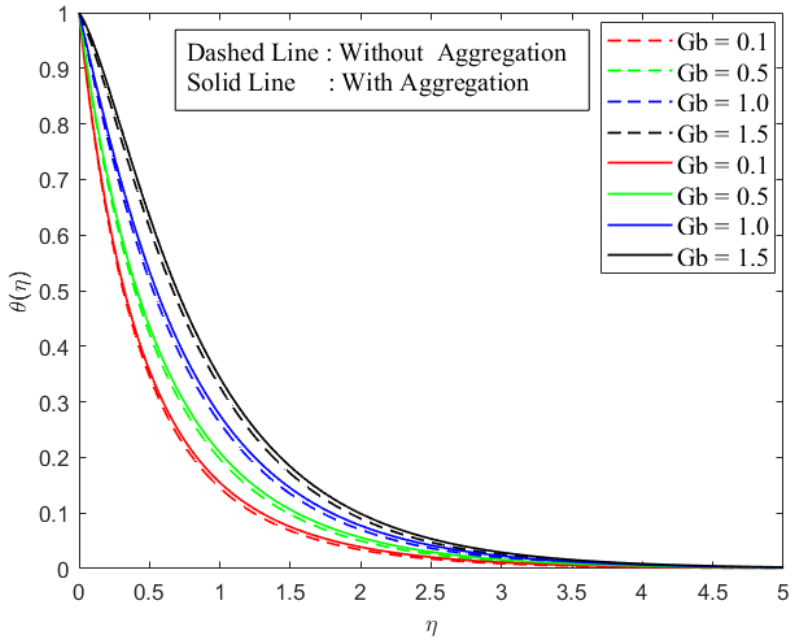

Figure 10. Variation of viscous dissipation parameter on temperature profile for $M = 1, E = 10^{-3}, R = 1, Pr = 5.83,$ $\phi = 0.1$

aggregated structures introduce additional resistance to the magnetic damping mechanism, thereby diminishing the overall influence of the Lorentz force on the flow. Consequently, the skin friction coefficient decreases with increasing magnetic parameters; the rate of reduction is lower in the presence of aggregation.

Fig. 12 illustrates the variation of the skin friction coefficient concerning the electric parameter E for both aggregated and non-aggregated nanoparticles. The analysis is conducted for three different values of the electric parameters that rise from 10^{-4} to 10^{-2}. It is evident from the graph that the skin friction coefficient decreases slightly with increasing electric parameters for both aggregation and non-aggregation cases. Notably, the presence of nanoparticles in aggregation leads

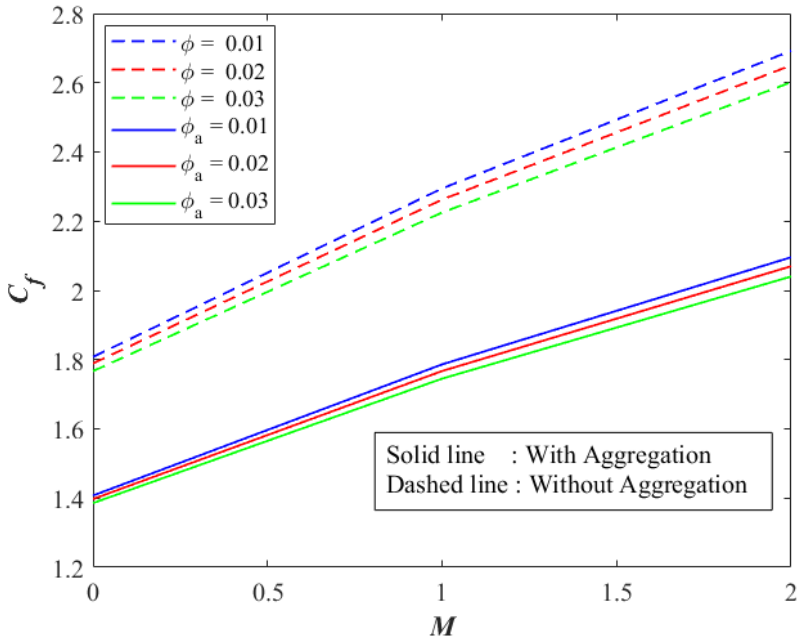

Figure 11. Variation of skin friction coefficient for increasing values of magnetic parameter for $E = 10^{-3}, R = 1, Pr = 5.83, Gb = 0.5$.

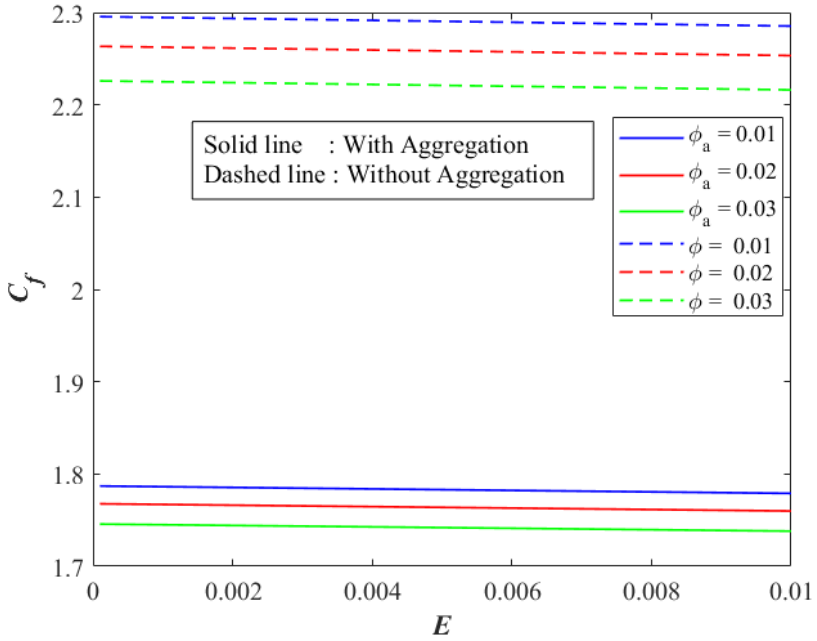

Figure 12. Variation of skin friction coefficient for increasing values of electric parameters for $M = 1, R = 1, Pr = 5.83, Gb = 0.5$.

to a consistently higher skin friction coefficient compared to the non-aggregated case. This indicates that aggregation increases the effective viscosity or momentum transfer near the wall, thereby increasing the resistance to flow.

The variation in the skin friction coefficient as a function of the radiation parameter R with volume fraction is evaluated for aggregated and non-aggregated nanoparticles shown in Fig. 13. It is observed that the skin friction coefficient remains almost constant across the entire range of the radiation parameters for both aggregated and non-aggregated. This behavior suggests that the radiation parameter has a negligible influence on the surface shear stress under the given flow conditions. This behavior indicates that nanoparticle aggregation enhances wall shear stress. Physically, this implies that the radiation-related energy transport does not significantly alter the momentum boundary layer thickness.

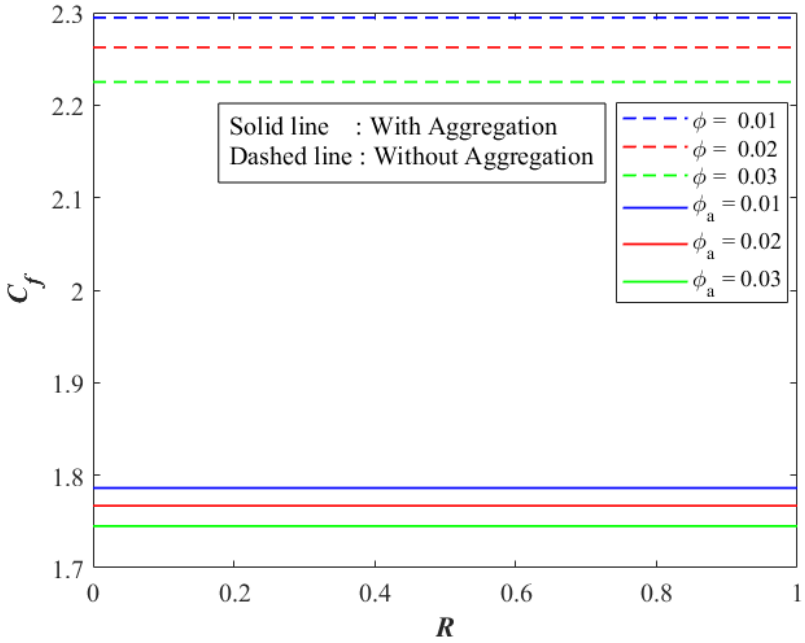

Figure 13. Variation of skin friction coefficient for increasing values of radiation parameter for $M = 1, E = 10^{-3}, Pr = 5.83, Gb = 0.5$.

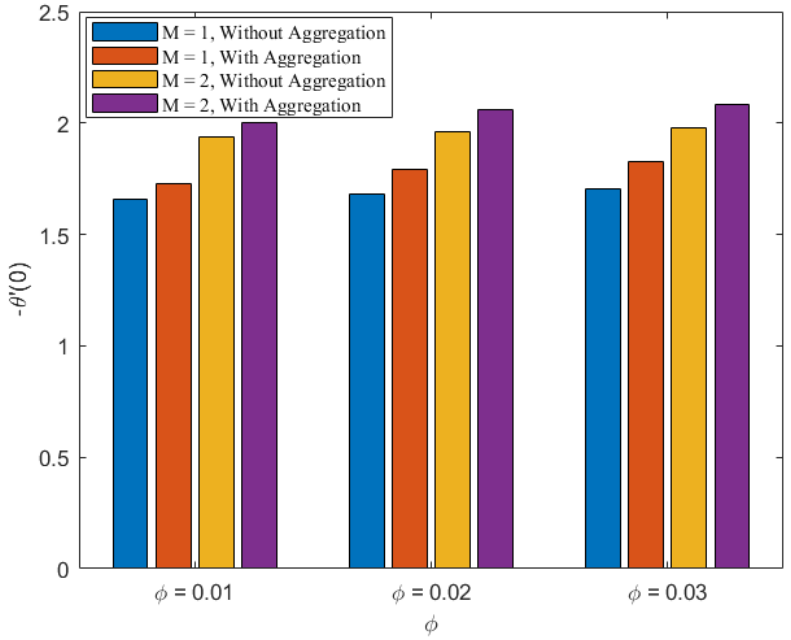

Figure 14. Behavior of heat transfer coefficient with increase in nanoparticle volume fraction for $E = 10^{-3}, R = 1.5, Pr = 5.83$ and $Gb = 1$.

The variation of the Nusselt number with respect to the magnetic parameter M for nanoparticle models with and without aggregation is shown in Fig. 14. An increase in the magnetic parameter results in a higher Nusselt number in both cases. In both magnetic field scenarios, the heat transfer coefficient with aggregation is consistently higher than the corresponding non-aggregated case. This can be attributed to the formation of nanoparticle clusters that facilitate superior thermal pathways and minimize interfacial resistance. The results emphasize that nanoparticle aggregation, along with higher volume fractions and stronger magnetic parameters, significantly augments the heat transfer performance of the nanofluid.

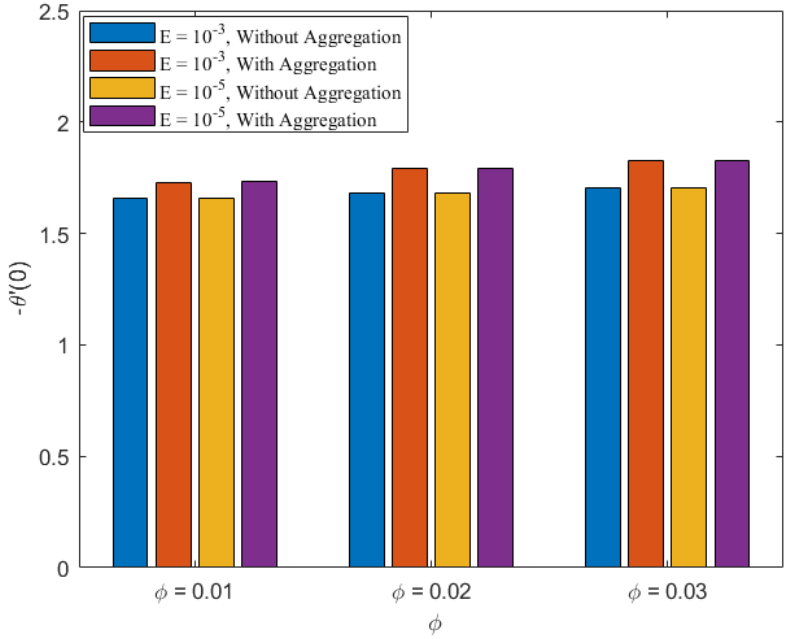

Figure 15. Behavior of heat transfer coefficient with increase in nanoparticle volume fraction for $M = 1, R = 1.5, Pr = 5.83$ and $Gb = 1$.

Fig. 15 demonstrates the Nusselt number increases with an increase in the values of the nanoparticle volume fraction for both aggregated and non-aggregated nanopartiles. The analysis reveals that as the electric parameter increases, the Nusselt number exhibits higher values in the presence of aggregated nanoparticles. Because the aggregated nanoparticle exhibits superior heat transfer performance compared to the non-aggregated case. The influence of the electric parameter is relatively mild, but at lower values of the electric parameter, the improvement due to aggregation remains consistent, indicating that aggregation effects dominate over changes in the electric parameter. Overall, the results confirm that nanoparticle aggregation amplifies the thermal transport, particularly at larger nanoparticle values.

7. CONCLUSION

The key contributions of the present study are summarized as follows:

- With an increasing magnetic parameter, the flow velocity of aggregated nanoparticles decreases by approximately 59% due to higher drag from larger clusters.
- Temperature profile increases in the presence of electric field for both aggregated and non-aggregated nanoparticles.
- The temperature rise is 15% higher for aggregated nanoparticles, indicating enhanced heat transfer due to aggregation effects.
- Increasing the radiation parameter raises the temperature profile with aggregated nanoparticles showing higher heat transfer due to enhanced radiation trapping and scattering within the aggregates.
- Electromagnetic effects improve heat transfer in the nanofluid, with aggregated nanoparticles exhibiting higher Nusselt numbers due to cluster formation that enhances thermal pathways.
- The nanoparticles aggregation model will be noticeable and more predominant than the homogeneous model due to its significant influence on the effective viscosity of the fluid.

8. PRACTICAL IMPLICATIONS

Aggregated nanoparticles in Cu/H_2O nanofluids significantly enhance heat transfer, with Nusselt numbers increasing under magnetic and electric fields, and higher radiation further improving thermal performance. Due to the nanoparticles aggregation, researchers and engineers can enhance heat transfer in nanofluid systems. Nanoparticles aggregation combined with enhanced thermal conductivity can significantly improve the efficiency of industrial thermal management systems, heat exchangers, and cooling devices.

9. RECOMMENDATIONS FOR FUTURE STUDIES

This study can be extended to future research based on nanofluid cooling systems for electric vehicles (EVs) by incorporating suction and injection at the boundaries to actively control flow and enhance heat transfer. The focus can be on how nanoparticle aggregation, shape, and size affect thermal performance under these conditions. By optimizing nanoparticle concentration, flow rates, and suction/injection strategies, the study can provide practical guidelines for designing efficient, high-performance EV thermal management systems that improve cooling efficiency while minimizing energy consumption.

ORCID

A. Lokeshwari, https://orcid.org/0009-0008-7591-9536; **Peri K. Kameswaran**, https://orcid.org/0000-0002-6357-7048

REFERENCES

[1] D. Lee, J.W. Kim, and B.G. Kim, "A new parameter to control heat transport in nanofluids: surface charge state of the particle in suspension," The Journal of Physical Chemistry B, **110**(9), 4323-4328 (2006). https://doi.org/10.1021/jp057225m.

[2] Gaganpreet, and S. Srivastava, "Effect of aggregation on thermal conductivity and viscosity of nanofluids," Applied Nanoscience, **2**(3), 325-331 (2012). https://doi.org/10.1007/s13204-012-0082-z.

[3] J. Liao, A. Zhang, S. Qing, X. Zhang, and Z. Luo, Z, "Investigation on the aggregation structure of nanoparticle on the thermal conductivity of nanofluids by molecular dynamic simulations," Powder Technology, **395**, 584-591 (2022). https://doi.org/10.1016/j.powtec.2021.10.007

[4] Y. Feng, B. Yu, P. Xu, and M. Zou, "The effective thermal conductivity of nanofluids based on the nanolayer and the aggregation of nanoparticles," Journal of Physics D: Applied Physics, **40**(10), 3164 (2007). https://doi.org/10.1088/0022-3727/40/10/020

[5] B. Mahanthesh, "Flow and heat transport of nanomaterial with quadratic radiative heat flux and aggregation kinematics of nanoparticles," International Communications in Heat and Mass Transfer, **127**, 105521 (2021). https://doi.org/10.1016/j.icheatmasstransfer.2021.105521

[6] J. Chen, C.Y. Zhao, and B.X. Wang, "Effect of nanoparticle aggregation on the thermal radiation properties of nanofluids: an experimental and theoretical study," International Journal of heat and mass transfer, **154**, 119690 (2020). https://doi.org/10.1016/j.ijheatmasstransfer.2020.119690

[7] M. Motevasel, A.R.S. Nazar, and M. Jamialahmadi, "The effect of nanoparticles aggregation on the thermal conductivity of nanofluids at very low concentrations: experimental and theoretical evaluations," Heat and Mass Transfer, **54**(1), 125-133 (2018). https://doi.org/10.1007/s00231-017-2116-2

[8] N. Muhammad, N. Ahmed, M. Rani, and B.B. Mohsin, "Application of deep learning to study aggregative and non-aggregative nanofluid flow within the nozzle of a liquid rocket engine," International Communications in Heat and Mass Transfer, **155**, 107449 (2024). https://doi.org/10.1016/j.icheatmasstransfer.2024.107449

[9] C. Pang, J.Y. Jung, and Y.T. Kang, "Aggregation based model for heat conduction mechanism in nanofluids," International Journal of Heat and Mass Transfer, **72**, 392-399 (2014). https://doi.org/10.1016/j.ijheatmasstransfer.2013.12.055

[10] R. Ellahi, M. Hassan, and A. Zeeshan, "Aggregation effects on water base Al2O3—nanofluid over permeable wedge in mixed convection," Asia-Pacific Journal of Chemical Engineering, **11**(2), 179-186 (2016). https://doi.org/10.1002/apj.1954

[11] P. Sathya, and P. Naveen, "Crucial role of nanoparticle aggregation effect on non-Darcian flow of micropolar nanofluid over Riga plate with Navier's slip: a regression analysis," The European Physical Journal Plus, **139**(5), 458, (2024). https://doi.org/10.1140/epjp/s13360-024-05230-y

[12] F.Z. Duraihem, "Electro-magnetohydrodynamic (EMHD) Darcy–Forchheimer flow of Sutterby nanofluid with variable thermal conductivity over a stretching sheet: Finite difference approach," Modern Physics Letters B, **39**(17), 2550019 (2025). https://doi.org/10.1142/S0217984925500198.

[13] K. Ramesh, K.K. Asogwa, T. Oreyeni, M.G. Reddy, and A. Verma, A, "EMHD radiative titanium oxide-iron oxide/ethylene glycol hybrid nanofluid flow over an exponentially stretching sheet," Biomass Conversion and Biorefinery, **14**(16), 18887-18896 (2024). https://doi.org/10.1007/s13399-023-04033-y

[14] V. Loganayagi, and P.K. Kameswaran, "Impacts of Heat Source/Sink and Electromagnetic Field on Heat Transfer in Ferrofluid Flow," Advances in Mathematics: Scientific Journal, **10**(4), 2095-2104 (2021). https://doi.org/10.37418/amsj.10.4.24

[15] J. Madhu, J.K. Madhukesh, K.V. Prasad, and A. Kulshreshta, "Exact solutions for nanoparticle aggregation and porous medium effects over a stretching surface," Multiscale and Multidisciplinary Modeling, Experiments and Design, **8**(2), 134 (2025). https://doi.org/10.1007/s41939-024-00724-9

[16] K. Swain, S.M. Ibrahim, G. Dharmaiah, G, and S. Noeiaghdam, "Numerical study of nanoparticles aggregation on radiative 3D flow of maxwell fluid over a permeable stretching surface with thermal radiation and heat source/sink," Results in Engineering, **19**, 101208 (2023). https://doi.org/10.1016/j.rineng.2023.101208

[17] P.K. Kameswaran, M. Narayana, P. Sibanda, and G. Makanda, "On radiation effects on hydromagnetic Newtonian liquid flow due to an exponential stretching sheet," Boundary Value Problems, **2012**(1), (2012). https://doi.org/10.1186/1687-2770-2012-105

[18] F. Wang, S.P. Rani, K. Sarada, R.P. Gowda, H.Y. Zahran, and E.E. Mahmoud, "The effects of nanoparticle aggregation and radiation on the flow of nanofluid between the gap of a disk and cone," Case Studies in Thermal Engineering, **33**, 101930 (2022). https://doi.org/10.1016/j.csite.2022.101930

[19] G.R. Rajput, B.P. Jadhav, and S.N. Salunkhe, "Magnetohydrodynamics boundary layer flow and heat transfer in porous medium past an exponentially stretching sheet under the influence of radiation," Heat Transfer, **49**(5), 2906-2920 (2020). https://doi.org/10.1002/htj.21752

[20] A. Ali, H.S. Khan, S. Saleem, S, and M. Hussan, M, "EMHD nanofluid flow with radiation and variable heat flux effects along a slandering stretching sheet," Nanomaterials, **12**(21), 3872 (2022). https://doi.org/10.3390/nano12213872

[21] K. Rafique, Z. Mahmood, A.M. Alqahtani, A.M. Elsiddieg, U. Khan, W. Deebani, and M. Shutaywi, "Impacts of thermal radiation with nanoparticle aggregation and variable viscosity on unsteady bidirectional rotating stagnation point flow of nanofluid," Materials Today Communications, 36, 106735 (2023). https://doi.org/10.1016/j.mtcomm.2023.106735

[22] F. Mabood, W.A. Khan, andA.M. Ismail, A, "MHD flow over exponential radiating stretching sheet using homotopy analysis method," Journal of King Saud University-Engineering Sciences, **29**(1), 68-74 (2017). https://doi.org/10.1016/j.jksues.2014.06.001

[23] B.M. Makhdoum, Z. Mahmood, B.M. Fadhl, M.S. Aldhabani, U. Khan, and S.M. Eldin, "Significance of entropy generation and nanoparticle aggregation on stagnation point flow of nanofluid over stretching sheet with inclined Lorentz force," Arabian Journal of Chemistry, **16**(6), 104787 (2023). https://doi.org/10.1016/j.arabjc.2023.104787

[24] J. Mackolil, and B. Mahanthesh, B, "Sensitivity analysis of Marangoni convection in TiO2–EG nanoliquid with nanoparticle aggregation and temperature-dependent surface tension," Journal of Thermal Analysis & Calorimetry, **143**(3), (2021). https://doi.org/10.1007/s10973-020-09642-7

[25] S.K. Rawat, M. Yaseen, A. Shafiq, M. Kumar, and Q.M. Al-Mdallal, "Nanoparticle aggregation effect on nonlinear convective nanofluid flow over a stretched surface with linear and exponential heat source/sink," International Journal of Thermofluids, **19**, 100355 (2023). https://doi.org/10.1016/j.ijft.2023.100355

[26] P. Rana, B. Mahanthesh, J. Mackolil, and W. Al-Kouz, "Nanofluid flow past a vertical plate with nanoparticle aggregation kinematics, thermal slip and significant buoyancy force effects using modified Buongiorno model," Waves in Random and Complex Media, **34**(4), 3425-3449 (2024). https://doi.org/10.1080/17455030.2021.1977416

ЧИСЛОВЕ ДОСЛІДЖЕННЯ АНАЛІЗУ ТЕПЛОПЕРЕНОСУ З ВИКОРИСТАННЯМ ЕЛЕКТРОМАГНІТОГІДРОДИНАМІКИ З АГРЕГОВАНИМИ НАНОЧАСТИНКАМИ

А. Локешварі, **Пері К. Камесваран**

Кафедра математики, Школа передових наук, Технологічний інститут Веллор, Веллор 632014, Індія

Оптимізація теплопередачі залишається суттєвою сучасною проблемою в сучасних технологічних застосуваннях. Нанорідини демонструють сильну потенційну теплопровідність для покращення теплопередачі та підвищення ефективності енергетичної системи. Порівняно з диспергованими наночастинками, агреговані наночастинки є важливими для оцінки теплової поведінки наночастинок у нанорівні. Незважаючи на цей ефект агрегації, фрактальна розмірність агрегованих наночастинок матиме трансформаційний вплив на теплопередачу. Метою цього дослідження є дослідження впливу електромагнітогідродинамічних ефектів на теплопередачу в нанорідині, що містить агреговані наночастинки над експоненціально розтягуваним шаром. Визначальні рівняння для імпульсу та енергії перетворюються на систему нелінійних звичайних диференціальних рівнянь із заданою межею умови. Представлено аналітичне рішення для конкретного випадку, коли параметр електричного поля відсутній. Чисельні рішення отримані для різних діапазонів фізичних параметрів, а обчислені результати перевірені на основі існуючої літератури. Результати показують, що агрегація наночастинок призводить до потовщення теплового граничного шару та покращення теплопередачі. На додаток до цього синергетичного ефекту агрегації та електричного поля, це призводить до зменшення профілів швидкості. При об'ємній частці 5% агреговані наночастинки забезпечують покращення теплопередачі приблизно на 34% порівняно з диспергованими наночастинками. Температурні профілі демонструють тенденцію до зростання зі збільшенням об'ємної частки. У присутності агрегованих наночастинок як коефіцієнт тертя поверхні, так і число Нуссельта збільшуються зі зростанням напруженості магнітного поля.

Ключові слова: *агреговані наночастинки; електричне поле; магнітне поле; випромінювання; в'язка дисипація; експоненціальне розтягування листа*